Progress and Prospects of Silicon-based Design for Optical phased array

Weiwei Hu[a], Chao Peng[a], Connie Chang-Hasnain [b]
[a]The State Key Laboratory of Advanced Optical Communication Systems and Networks, School of Electronics Engineering and Computer Science, Peking University, Beijing 100871, China;
[b]Department of Electrical Engineering and Computer Sciences, University of California at Berkeley, California, CA 94720, USA

ABSTRACT

The high-speed, high-efficient, compact phase modulator array is indispensable in the Optical-phased array (OPA) which has been considered as a promising technology for realizing flexible and efficient beam steering. In our research, two methods are presented to utilize high-contrast grating (HCG) as high-efficient phase modulator. One is that HCG possesses high-Q resonances that origins from the cancellation of leaky waves. As a result, sharp resonance peaks appear on the reflection spectrum thus HCGs can be utilized as efficient phase shifters. Another is that low-Q mode HCG is utilized as ultra-lightweight mirror. With MEMS technology, small HCG displacement (~50 nm) leads to large phase change (~1.7 π). Effective beam steering is achieved in Connie Chang-Hasnian's group. On the other hand, we theoretically and experimentally investigate the system design for silicon-based optical phased array, including the star coupler, phased array, emission elements and far-field patterns. Further, the non-uniform optical phased array is presented.

Keywords: high-contrast grating, optical phased array, beam steering, high-Q resonance

1. INTRODUCTION

Optical-phased array (OPA) has been considered as a promising technology for realizing flexible and efficient beam-steering that avoids mechanical moving parts. Through manipulating the phases of individual array unit, the propagating direction and field pattern of the outgoing beam can be tuned accordingly. Therefore, OPA can be potentially utilized in various application, including optical wireless communication and integrated display.

Among OPA, a compact, high-speed, high-efficient phase modulator array is one of key components. With the development of silicon photonic technology, the silicon-on-insulate (SOI) become promising platform to realize integrated phase modulator. In our research, we propose to utilize high-contrast grating (HCG) as phase modulator. It is proved that HCG possesses high-Q resonances that origins from the interfering of resonance waves. As a result, sharp peaks appear on the reflection spectrum, which can be adopted to realize efficient phase shifters. We proposed a semi-analytical model to depict the behavior of electromagnetic field within the HCGs. The high-index contrast, which weakens the validity of the perturbation assumption that was applied in some conventional models, has been properly treated in our semi-analytical model. Thus we can perform a systematic optimization of HCG devices. Moreover, the reflection spectrum has been observed from our measurement system, to confirm the findings of high-Q resonances within HCG.

Another OPA scheme in which the low-Q HCGs have been adopted as broadband mirror is investigated in Connie's group. A high speed novel 8x8 optical phased array based on high contrast grating all-pass filters with low voltage microelectromechanical actuation is demonstrated. Each array element is an all-pass filter (APF) at 1550 nm with a HCG as a reflective top reflector and a distributed Bragg reflector (DBR) as the bottom reflector. The incident light comes at surface normal to the APF; the phase of the reflective light can be tuned efficiently with a small actuation distance of the HCG. Beam steering is demonstrated by creating a near-field reflection phase pattern with different actuation voltages on individual pixels.

High Contrast Metastructures V, edited by Connie J. Chang-Hasnain, David Fattal, Fumio Koyama, Weimin Zhou, Proc. of SPIE Vol. 9757, 97570U · © 2016 SPIE
CCC code: 0277-786X/16/$18 · doi: 10.1117/12.2214155

On the other hand, we also propose another system scheme of OPA in which conventional silicon waveguide phases modulator are designed and the HCGs have been utilized as optical antenna. We theoretically and experimentally investigate the system design including the star coupler, phased array, emission elements and far-field patterns.

2. OPTICAL PHASED ARRAY BASED ON HIGH-CONTRAST GRATING

2.1 HCG with high-Q Resonance

A HCG is schematically shown in Fig. 1. High index refractive dielectric bars (typically silicon) are surrounded by low refractive index material (air in most cases). HCG structure can be described by following parameters: the period (Λ), duty cycle (DC), thickness of gratings (t_g), and refractive index of dielectric (n). The HCG is essentially a subwavelength grating, i.e., the incident wavelength is larger than the grating period. Therefore, all non-zero order diffraction modes of the grating are evanescent, and only the 0th-order mode is able to radiate outside the grating[1,2].

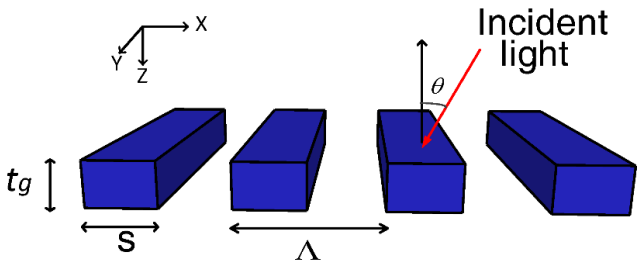

Figure 1. Schematic of an HCG, the blue bar illustrate the grating.

The HCG can be regarded as a dielectric waveguide with periodic modulated refractive index. On phase matching condition, two counter propagating waves dominate the energy inside the grating, referred to as "basic waves". These two basic waves share the same absolute value of wave vector, but propagate in opposite directions. When they are in phase, the constructive interference makes the energy radiates out through 0th order diffraction easily, results in the low-Q mode. On the contrary, when basic waves are out of phase, they interfere destructively. For a horizontally symmetric HCG, the corresponding radiative waves of cancel each other out, leading to the high-Q mode. In this case, no energy radiates out of the grating[3]. Therefore, the high-Q mode bandwidth on the transmissivity/reflectivity spectrum is extremely narrow. Hence, this mode becomes a promising candidate for an efficient phase shifter. In practical cases, defects or limited length of HCG will lead to finitely high Q mode. Here we assume a slightly oblique incident light to illustrate the typical spectrum of HCG device, as shown in Fig. 2.

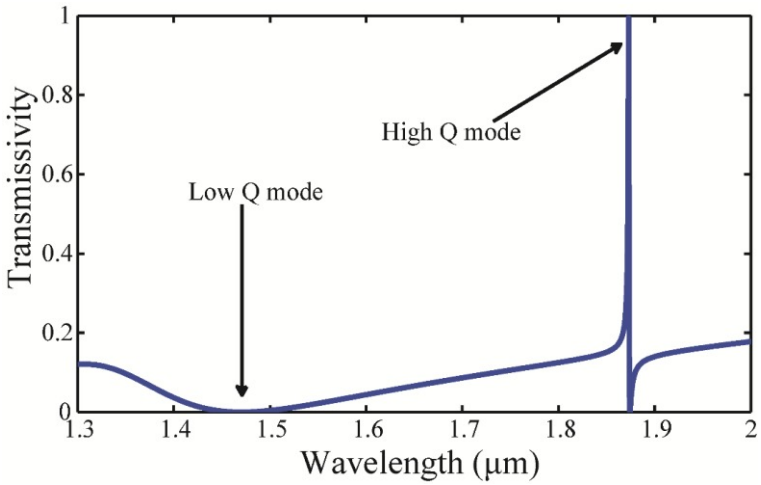

Figure 2. Typical spectrum of HCG calculated with RCWA (DC=0.45, t_g=0.22 μm, n=3.48, Λ=1 μm, θ=2°).

The bandwidth of the high-Q mode is ultra-narrow. At the same time the central wavelength of the high Q mode is affected by many factors, including the duty cycle, period, refractive index of dielectric, and incident angle. Consequently, this HCG can be applied in varieties of optoelectronic devices, including ultra-wideband filters and

reflector[4,5], tunable vertical-cavity surface-emitting lasers (VCSELs)[6], high-Q optical resonators, and hollow-core waveguides (HW)[7].

2.2 Analysis of HCG based Phase Shifters

We propose to use HCG as phase shifters, by utilizing its high Q resonance. With RCWA method, the relationship between the central wavelength of resonance peak and the refractive index of dielectric is numerically investigated. We found that the central wavelength increases when the refractive index of the dielectric slab increases. Analysis over a large number of the parameters indicates that the ratio $d\lambda/dn$ mainly depends on the refractive index. For silicon gratings, the central wavelength changes about 0.4 nm when the refractive index change of 0.001 is applied. The reflectivity or transmissivity of the resonance mode can be expressed with Lorentz Function.

$$t = \frac{\exp(i\varphi_0)}{1 + i(\lambda - \lambda_0)/w} \tag{1}$$

Here λ_0 is the central wavelength, φ_0 is the phase shift at the central wavelength, and $2|w|$ is the full width at half maximum (FWHM). According to characteristics of HCG, the Q-factor and wavelength of the high Q mode is depended on incident angle, defect, limited length, and HCG geometry parameters. Applying these rules to a non-radiative resonance mode, the bandwidth and central wavelength can be designed and engineered to desire values.

The change of central wavelength $d\lambda_0$ leads to the transmitted light at resonance peak possessing a phase shift and loss, given by the following equations:

$$\frac{d\varphi}{d\lambda_0} = \frac{1}{w} \tag{2}$$

$$\left|t^2\right| \approx 1 - \frac{d\lambda_0^2}{w^2} \tag{3}$$

And hence, the loss can be written as

$$loss(dB) \approx 10\log_{10}\frac{d\lambda_0^2}{w^2} \tag{4}$$

Suppose the phase shift is $\Delta\varphi$, Eq. (2) and (4) gives $\Delta\lambda_0 = \Delta\varphi w$ and the loss (dB) $\approx 10\Delta\varphi^2/\ln 10$, therefore, the loss of the transmitted light quadratic growth with the phase shift. A sample design of phase shifter is shown in Fig. 3. The bandwidth of the phase shifter is 4.4 pm. When assuming a small refractive index increased of 1.0×10^{-5}. The corresponding central wavelength shift is about 3.8 pm, and the phase shift of 1.25 rad is provided.

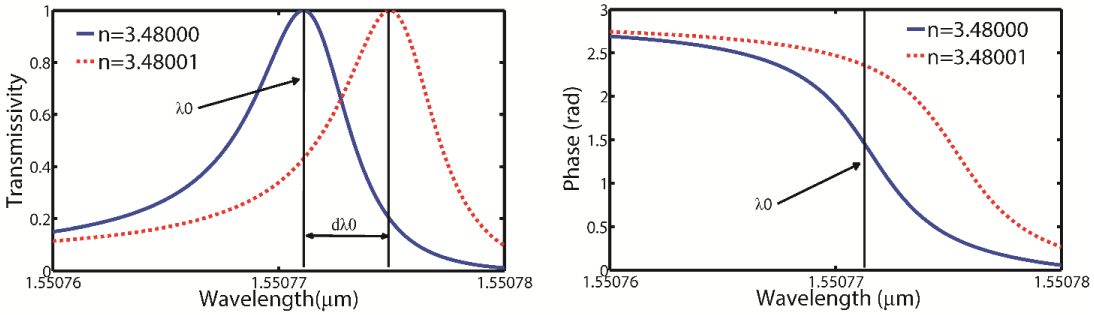

Figure 3. An example of HCG phase shifter (DC=0.329, t_g=0.228 μm, period=0.98 μm, θ=0.1°)

2.3 Experimental Observation of High-Q mode

We established a HCG normal incident reflectivity spectrum measurement system, as shown in Fig. 4. The measurement system mainly consists of four parts: incidence part, reflection part, sample observation part and output measurement part. Laser light is incident into the system through a fiber collimator, focused on the sample by a microscope objective lens. The reflected light amplitude is transferred into voltage by the photodiode, observed on an oscilloscope and measured with digital data acquisition device.

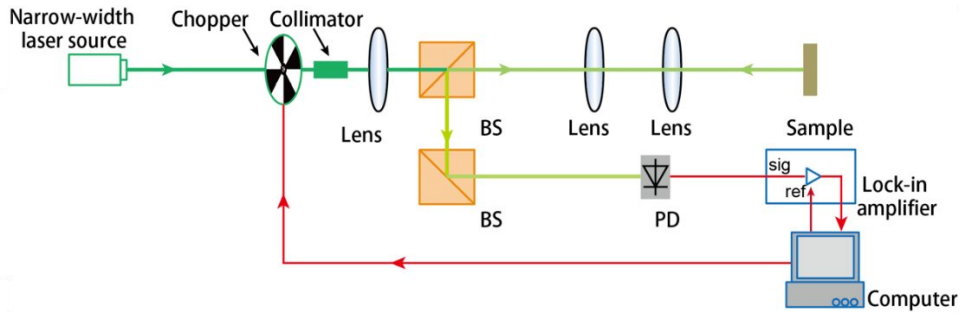

Figure 4. Main part of the reflectivity spectrum measurement system.

With this system, the reflectivity spectrum of HCG sample is able to be measured. High Q mode is obvious on the spectrum, as shown in Fig. 5.

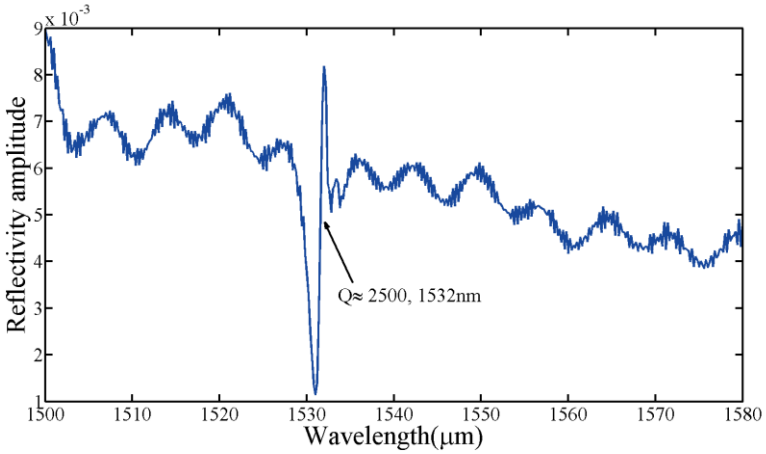

Figure 5. HCG high Q mode reflectivity spectrum measured by our system

System scheme of HCG resonance based OPAAs mentioned above, phase shifter can be achieved with HCG, by utilizing its high Q resonance property. Further, placed in the form of an array and working under certain condition, HCG resonance phase shifters behave as an Optical Phased Array. HCG units in different positions of the OPA, may be modulated through changing separate refractive index conditions, and consequently, add different phase shift onto the incident light, leading to a deflection of the reflected light. A schematic design of resonance HCG based OPA is shown in Fig. 6.

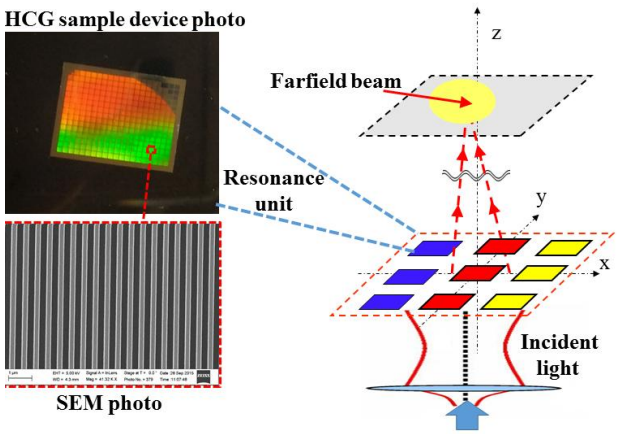

Figure 6. HCG high Q mode reflectivity spectrum measured by our system

2.4 HCG-APF OPA

OPA can also be realized through MEMS technology[8,9]. By utilizing the HCG low-Q mode character, i.e., broadband high reflectivity, Prof. Connie Chang-Hasnian's group experimentally demonstrated highly effective OPA, with fast response time(< 4 microseconds), large field of view(±2 °) and narrow beam divergence(0.1 °)[10]. In this solution, HCG is utilized as ultra-lightweight mirror. With MEMS technology, small HCG displacement (~50 nm) leads to large phase change (~1.7 π)[11]. Therefore, effective beam steering is achieved.

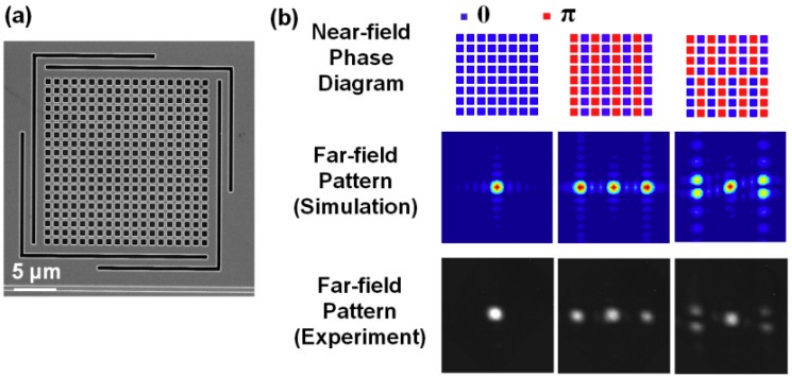

Figure 7. (a) SEM image of the two-dimensional HCG mirror. (b) Beam steering experiment of the optical phased array using two-dimensional HCG as the top mirrors. Top panel, near-field phase pattern created by the optical phased array. Middle panel, the corresponding far-field pattern calculated by Fourier optics. Bottom panel, experimentally measured far-field pattern, in good agreement with the calculation[11]

3. SYSTEM DESIGN OF SILICON-BASED OPTICAL PHASED ARRAY

The typical structure of OPA system can be mainly divided into three parts by function: beam splitter, phase shifters and grating array. Considering of large-scale integration and system performance optimization, star coupler, electro-optical (EO) modulators and grating array are introduced to form the silicon-based OPA system. Fig. 8 shows the system structure of the silicon-based optical phased array.

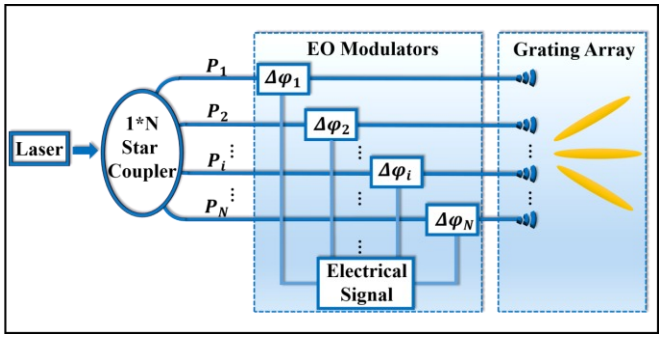

Figure 8. System structure of the silicon-based optical phased array

3.1 Star coupler

The traditional OPA system generates the far-field waveform by adjusting the phase shifters part only while the amplitude of emission elements is uniform. However, phase control alone is not enough for beam forming since one optical field includes phase as well as amplitude. Here in our proposal, the freedom of amplitude control is added in beam splitter part in order to optimize the far-field waveform.

For the purpose of amplitude control and large-scale integration, 1 ×N star coupler is introduced instead of multimode interference (MMI) or cascaded Y-branch optical coupler which are commonly used in on-chip OPA systems. Star coupler have more adjustable parameters to shape output amplitude distribution and can splitter beam directly without cascaded structure.

Then we turn to engineer the output amplitude distribution of star coupler to achieve better far-field waveform. Base on the Fourier optics, the relation between the near-field wave front and the far-field wave front is proved to hold as a Fourier transform pair[12] and the uniform distribution of the near-field wave front can be regarded as the rectangular window. The side lobes of far-field wave front are caused by the rectangular window which is cut off sharply. So we need to find slowly varying distribution function to suppress the side lobes with specified width of main lobe.

C. L. Dolph has presented a means of improving the pattern of linear antenna arrays based on the properties of the Tchebyscheff polynomials by which the side-lobe level can be minimized when the first null is specified[13]. This algorithm is applied to optical domain and deduce Dolph's calculation to change the condition from specified first null to specified half-power point for our demand. After using the improved Tchebyscheff algorithm to get amplitude distribution, the apodization of the near-field is achieved and the simulation result of 1×16 OPA in Fig. 9(a) shows a side-lobe level decrease of nearly 18 dB while the FWHM shows slight increase from 1.64 °to 2.08 °. Fig. 9(b) illustrates the side-lobe level with uniform amplitude distribution and Tchebyscheff apodization amplitude distribution when the number of array elements increases. It shows the decrease of side-lobe level is about 17 dB on average.

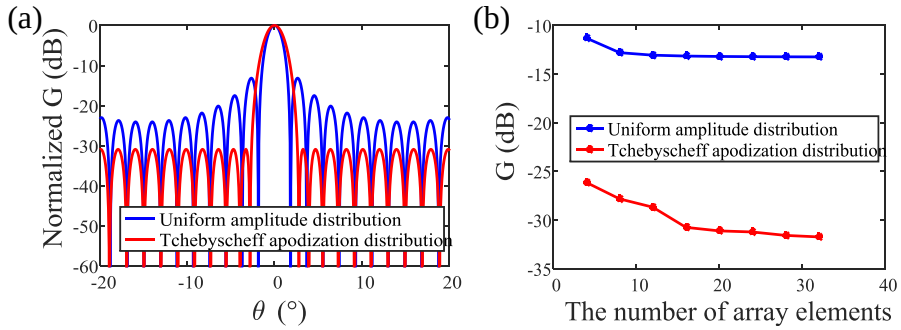

Figure 9. (a)The far-field waveform simulation result of a 1×16 OPA. A side-lobe reduction of nearly 18 dB can be seen. (b) The comparison of side-lobe level with uniform amplitude distribution and Tchebyscheff apodization amplitude distribution when the number of array elements increases.

Based on the optimized amplitude distribution, we begin to design the star coupler using the structure which was firstly mentioned by C.Dragone[14]. By adjusting parameters using beam propagation method (BPM), we can achieve the Tchebyscheff apodization amplitude distribution deduced above. Fig. 10(a) shows the simulation result of designed star coupler by BPM. The star coupler was realized on SOI with the top silicon layer 220 nm-thick and the buried oxide layer 1-μm thick. The total size is about 40 μm ×60 μm. Fig. 10(b) shows the SEM images of the device details. The star coupler was tested on a standard integrated optics setup with a tunable laser. Fig. 10(c) shows the near-field pattern of the light from the output spots, where the amplitude distribution decreases from the center to the edge as design. Fig. 10(d) reveals the average amplitude measurement results of 16 outputs, which are very closed to the designed distribution. Moreover, the insert loss of the designed star coupler was less than 1 dB which is much lower than other tunable optical coupler structure.

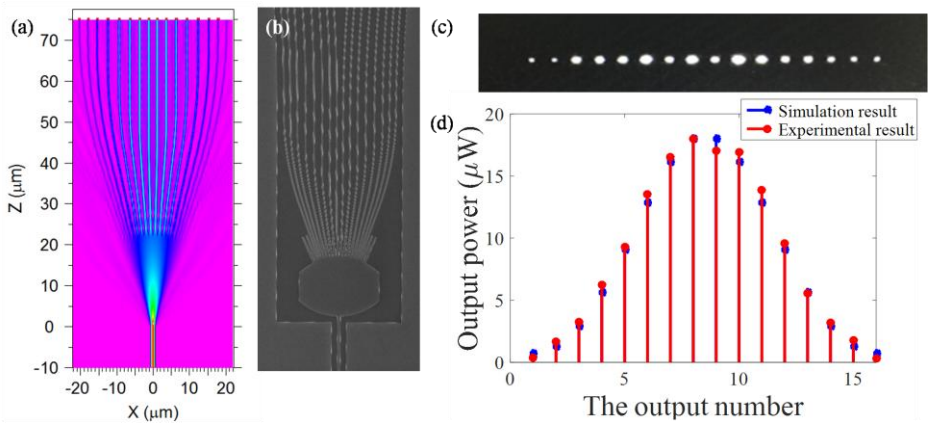

Figure 10. (a) The simulation result of designed star coupler by 3D-BPM. (b) SEM images of the fabricated star coupler. (c)The near-field pattern of the light from the output spots. (d) The average amplitude measurement results of outputs.

3.2 Phase shifter

To obtain a small chip size and maintain a considerable array number, we need phase shifters with high modulation efficiency. Considering the high thermo-optical coefficient (TOC) of silicon, it's natural to employ thermo-optical effect to phase shifting[15,16]. Nevertheless, due to its protracted response time, the speed of the whole system is limited to about 100 kHz, which is far from industrial practicability. In the meantime, typical electro-optical (EO) modulator is focused more on speed. Thus carrier-depletion structure is widely used to achieve a broad bandwidth[17], yet the length to shift π phase is too tremendous to form a large scale. To meet the requirements of OPA systems and seek for a balance between bandwidth and efficiency, we've chosen a p-i-n carrier-injection structure as our phase shifter and optimized the phase shifter on a 220 nm SOI platform.

The simulating calculation is under 2-D device simulation package SILVACO and Finite-difference time-domain (FDTD) methods. Fig.11 (a) illustrates the cross-section of the optimized result. The 600nm-wide rib with 130nm etched slab on each side is designed to satisfy the single mode condition at $\lambda = 1550nm$. The width W between rib waveguide and doped region is a key factor to design. Greater W increases the carrier drifting time and brings a bigger junction capacitance, causing a decreasing of bandwidth and a gaining of extra energy loss. While smaller W leads to a larger light consumption and may cause a thermo-optical cross-talk in different channels. The modeling results also predict that the transient performance of the device is affected significantly by the contact width. To diminish the thermal influence and guarantee a fair response time, the contact width is set at 9.5 μm.

R.A.Soref calculated the expressions relating the refractive index and absorption coefficients changes of silicon. At $\lambda = 1550nm$, it was given as follow[18], in which Δn_e and Δn_h is the change in refractive index resulting from change in free electron-carrier concentrations and from change in free hole-carrier concentrations; $\Delta\alpha_e$ and $\Delta\alpha_h$ is the change in absorption resulting from change in free electron-carrier concentrations and change in free hole-carrier concentrations:

$$\Delta n = \Delta n_e + \Delta n_h = -[8.8 \times 10^{-22}\Delta N_e + 8.5 \times 10^{-18}(\Delta N_h)^{0.8}]$$

$$\Delta\alpha = \Delta\alpha_e + \Delta\alpha_h = 8.5 \times 10^{-18}\Delta N_e + 6.0 \times 10^{-18}\Delta N_h$$

Combining the expressions above with SILVACO simulation, we can predict a 2π phase shift in the length of 200 μm and at the voltage of 0.95 V, ensuring a similar small size as thermo-optical solutions. At the same time, a transient time analysis is given in Fig. 4 (b) the electrical pulse is given at t = 10 ns and removed at t = 100 ns. It shows that the main limit is due to the rise time τ_r, which is a response of carriers being injected to the intrinsic region and recombining. Under the thermal-safe circumstance, the calculated bandwidth is 47 MHz, which is hundreds of times faster than the existing thermo-optical results.

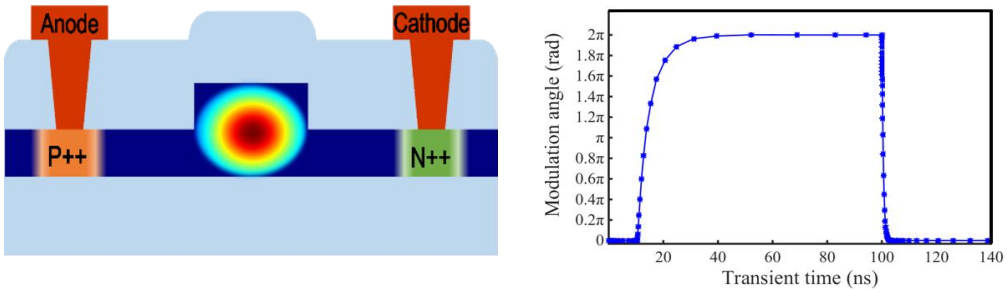

(a) (b)

Figure 11. (a) Cross-section through active region of the phase shifter on 220 nm SOI platform.(b) Calculated transient performance for the reference modulator. The electrical pulse is given at t = 10 ns and removed at t = 100 ns.

3.3 Antenna array design

The HCGs have been utilized as optical antenna. Beam emission is achieved by a curved HCG array[15]. Each element is curved in order to reduce the length of the taper between waveguide and grating. The emitter measures 3.0 μm in length, 2.8 μm in width. By optimizing the period, duty cycle, and etch depth of the curved grating coupler, the 3D FDTD

simulation results show that the maximum radiation efficiency of an curved element is 67% at a central wavelength 1550 nm.

Due to the limitation of silicon waveguides width, element spacing d cannot meet zero-side-lobe condition $d < \lambda / 2$ (λ is optical wavelength). Thus an irregularly spacing array is designed to decrease side lobe[19] which is a main difficulty that impede OPA beam steering from achieving high performance and practical application.

Using greedy method to calculate emitter spacing, an 8×8 OPA nonuniform spacing output array is shown in Fig. 12. Each inserted emitter spacing is calculated to vanish the most powerful side lobe. With emitter number added, a set of optimized spacing which form an irregularly sequence are gained. Fig. 12(a) and Fig. 12(b) manifest that the nonuniform spacing array can decrease impact of side lobe efficiently. In a 2D OPA, nonuniform spacing optimized by greedy method can ensure more centeredlight intensity, and then achieve a wide range beam scanning.

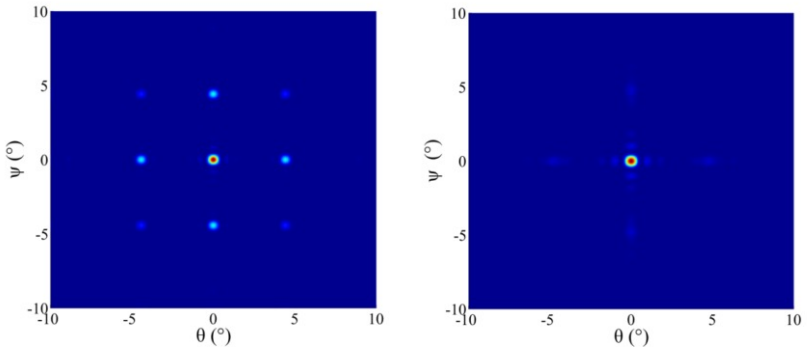

Figure 12. Far-field interference pattern of 8×8 array of (a) uniform spacing design and (b) nonuniform spacing design.

4. SUMMARY

In summary, the HCG devices for high-Q mode and low-Q mode are investigated theoretically and experimentally. The experiment shows that a high-Q HCG device of about 2500 at 1532 nm is obtained. An example of HCG phase shifter shows that the phase shift of 1.25 rad is provided if the corresponding central wavelength shifting about 3.8 pm.

A novel 8x8 optical phased array using HCG-APF is experimentally demonstrated for beam steering. The key advantage of using HCG APF is its high efficient phase tuning, i.e. small HCG MEMS mirror displacement (~50 nm) for large phase change (~1.7 π), and small voltage actuation (10 V) for fast beam steering (>0.5 MHz).

An advanced conventional silicon-based OPA scheme is investigated, in which the waveguide amplitude and phase modulator are designed and the HCGs have been utilized as optical antenna. The freedom of amplitude control is nearly no loss added in beam splitter design. After using the improved Tchebyscheff algorithm to get amplitude distribution, the apodization of the near-field is achieved and the simulation result of 1×16 OPA shows a side-lobe level decrease of nearly 18 dB. A p-i-n carrier-injection structure is chosen as the phase shifter which is hundreds of times faster than the existing thermo-optical results. The HCGs have been utilized as optical antenna. Simulation shows that the maximum radiation efficiency of 67% at a central wavelength 1550 nm is obtained for a curved HCG element. Furthermore, in a 2D OPA, nonuniform spacing optimized by greedy method decreases impact of side lobe efficiently.

ACKNOWLEDGEMENTS

This work was supported by the National Natural Science Foundation of China (NSFC) under Grant 61320106001, the Specialized Research Fund for the Doctoral Program of Higher Education under Grant 20120001110094, and the State Key Laboratory of Advanced Optical Communication Systems and Networks, China.

REFERENCES

[1] Chang-Hasnain, C. J., & Yang, W., "High-contrast gratings for integrated optoelectronics," Advances in Optics and Photonics, 4(3), 379-440 (2012).

[2] Karagodsky, Vadim, F. G. Sedgwick, and C. J. Chang-Hasnain. "Theoretical analysis of subwavelength high contrast grating reflectors," Optics Express, 18(16), 16973-16988 (2010).

[3] Yang, Y., Peng, C., Liang, Y., Li, Z., and Noda, S., "Analytical perspective for bound states in the continuum in photonic crystal slabs," Physical review letters, 113(3), 037401 (2014).

[4] Y. Zhou, M. Huang, C. Chase, V. Karagodsky, M. Moewe, B. Pesala, F. Sedgwick, and C. Chang-Hasnain, "High-index-contrast grating (HCG) and its applications in optoelectronic devices," IEEE Journal of Selected Topics in Quantum Electronics 15, 1485–1499 (2009).

[5] M. C. Y. Huang, Y. Zhou, and C. J. Chang-Hasnain, "A surface-emitting laser incorporating a high-index-contrast subwavelength grating," Nature Photonics 1, 119–122 (2007).

[6] Y. Zhou, M. C. Y. Huang, and C. Chang-Hasnain, "Large fabrication tolerance for VCSELs using high-contrast grating," IEEE Photonics Technology Letters 20, 434 –436 (2008).

[7] C. F. R. Mateus, M. C. Y. Huang, L. Chen, C. J. Chang-Hasnain, and Y. Suzuki, "Broad-band mirror (1.12-1.62 um) using a subwavelength grating," IEEE Photonics Technology Letters 16 (2004).

[8] Bifano, T. G., Perreault, J., Mali, R. K., and Horenstein, M. N., "Microelectromechanical deformable mirrors," Selected Topics in Quantum Electronics, IEEE Journal of, 5(1), 83-89 (1999).

[9] Krishnamoorthy, U., Li, K., Yu, K., Lee, D., Heritage, J. P., and Solgaard, O., "Dual-mode micromirrors for optical phased array applications," Sensors and Actuators A: Physical, 97, 21-26 (2002).

[10] Yoo, B. W., Megens, M., Chan, T. K., Sun, T., Yang, W., and Horsley, D. A., et al., "32×32 Optical phased array with ultra-lightweight high-contrast-grating mirrors," Solid-State Sensors, Actuators and Microsystems (TRANSDUCERS & EUROSENSORS XXVII), 2013 Transducers & Eurosensors XXVII: The 17th International Conference on. IEEE, 144-5 (2012).

[11] Yang, W., Sun, T., Rao, Y., Megens, M., Chan, T., Yoo, B. W., and Chang-Hasnain, C. J., "High speed optical phased array using high contrast grating all-pass filters," Optics express, 22(17), 20038-20044 (2014).

[12] Goodman, J. W., "Introduction to Fourier optics, " Roberts and Company Publishers (2005).

[13] Dolph, C. L., "A current distribution for broadside arrays which optimizes the relationship between beam width and side-lobe level, " Proceedings of the IRE, 34(6), 335-348 (1946).

[14] Dragone, C., Henry, C. H., Kaminow, I. P., & Kistler, R. C., "Efficient multichannel integrated optics star coupler on silicon," Photonics Technology Letters, IEEE, 1(8), 241-243(1989).

[15] Sun, J., Timurdogan, E., Yaacobi, A., Hosseini, E. S., & Watts, M. R., "Large-scale nanophotonic phased array, " Nature, 493(7431), 195-199(2013).

[16] Van Acoleyen, K., Bogaerts, W., Jágerská, J., Le Thomas, N., Houdré, R., & Baets, R., "Off-chip beam steering with a one-dimensional optical phased array on silicon-on-insulator, " Optics letters, 34(9), 1477-1479(2009).

[17] Hosseini, S., & Jamshidi, K., "Circuit modeling based optimization of high speed carrier depletion silicon modulators," In SPIE Optics+ Optoelectronics (pp. 95160N-95160N). International Society for Optics and Photonics(2015).

[18] Soref, R. A. & Bennett,B. R., "Kramers-Kronig analysis of E-O switching in silicon, " SPIE Integrated Opt. Circuit Eng., vol. 704, pp. 32–37(1986).

[19] Xiao F, Hu W, Xu A., "Optical phased-array beam steering controlled by wavelength," Applied Optics, 44(26):5429-5433(2005).